

A Ghost Story II: Ghosts, Gluons and the Gluon condensate beyond the IR of QCD

J. Rodríguez-Quintero*

Dpto. Física Aplicada, Huelva †

E-mail: jose.rodriguez@dfaie.uhu.es

Ph. Boucaud, J.P. Leroy, A. Le Yaouanc, J. Micheli, O. Pène

LPT Orsay (CNRS) ‡

E-mail: philippe.boucaud@th.u-psud.fr,
leroy@th.u-psud.fr, leyaouan@th.u-psud.fr,
micheli@th.u-psud.fr, olivier.pene@th.u-psud.fr

F. De Soto

U.P.O., Sevilla

E-mail: fcsotobor@upo.es

Beyond the deep IR, the analysis of ghost and gluon propagators still keeps very interesting non-perturbative information. The Taylor-scheme coupling can be computed and applied to obtain the Λ_{QCD} parameter from Landau gauge lattice simulations. Furthermore, a dimension-two gluon condensate, that can be understood in the instanton liquid model, plays an important role in the game.

*International Workshop on QCD Green's Functions, Confinement and Phenomenology
September 7-11, 2009
ECT Trento, Italy*

*Speaker.

†Fac. Ciencias Experimentales, Universidad de Huelva, 21071 Huelva, Spain

‡^aLaboratoire de Physique Théorique, Unité Mixte de Recherche 8627 du Centre National de la Recherche Scientifique Université de Paris XI, Bâtiment 210, 91405 Orsay Cedex, France

1. Introduction

Much work has been devoted in the last years to the study of the QCD running coupling constant determined from lattice simulations, as well in its perturbative regime [1–9] as in the deep infrared domain [10]. Only very recently [9, 11], the Green’s function approach to study the running coupling and then to estimate $\Lambda_{\overline{MS}}$ has been pursued by exploiting a non-perturbative definition of the coupling derived from the ghost-gluon vertex. The very infrared domain for the running of the coupling so defined has been discussed in the Olivier Pene’s talk. We aim to deal here with the running behaviour of this ghost-gluon coupling beyond the IR domain, above roughly 2-3 GeV.

We will show that the analysis of *quenched* lattice simulations leads to a non-perturbative determination of the running coupling in terms of two-point ghost and gluon Green functions and to obtain $\Lambda_{\overline{MS}}$ in pure Yang-Mills ($N_f = 0$). Furthermore, a very realistic estimate of $\Lambda_{\overline{MS}}$, directly comparable with experimental determinations, will become an immediate possibility thanks to the many unquenched configurations which are presently available.

A precise determination of the non-perturbative coupling from the lattice also reveals a dimension-two non-zero gluon condensate in the Landau gauge [10]. One needs then to describe the running with a formula including non-perturbative power corrections to be confronted with lattice estimates of the coupling. This procedure constitutes an optimal method for the identification of $\Lambda_{\overline{MS}}$ and of the gluon condensate [11]. Much work has been also done to investigate its phenomenological implications in the gauge-invariant world [12]. In particular, we will discuss the interpretation of this condensate in terms of the Yang-Mills semiclassical field background by applying the Instanton liquid model.

2. The ghost-gluon coupling

There is a large number of possibilities to define the QCD renormalized coupling constant, depending on the observable used to measure it and on the renormalization scheme. Actually, any observable which behaves, from the perturbative point of view, as g provides a suitable definition for it. Among such quantities stand the 3-gluon and the ghost-gluon vertices, which have been widely used by the lattice community to get a direct knowledge of α_s from simulations. Of course an important criterion to choose among those definitions will be how easy it is to connect it to other commonly used definitions, specially the \overline{MS} one, and to extract from it fundamental parameters like Λ_{QCD} .

A convenient class of renormalization schemes to work with on the lattice is made of the so-called *MOM* schemes which are defined through the requirement that a given scalar coefficient function of the Green’s function under consideration take its tree-level value in a specific kinematical situation given up to an overall “renormalization scale”. To make the point clearer we recall 2 schemes which we have used in previous works on α_s :

- The symmetric 3-gluon scheme in which one uses the 3-gluon vertex $\Gamma_{\mu\nu\rho}(p_1, p_2, p_3)$ with $p_1^2 = p_2^2 = p_3^2 = \mu^2$
- The asymmetric 3-gluon scheme (\widetilde{MOM}) in which the 3-gluon vertex $\Gamma_{\mu\nu\rho}(p_1, p_2, p_3)$ is used with $p_1^2 = p_2^2 = \mu^2, p_3^2 = 0$

In the present note we shall apply a specific *MOM*-type renormalization scheme defined by fixing the (ghost and gluon) propagators and the ghost-gluon vertex at the renormalization point. Let us start by writing the ghost and gluon propagators in Landau gauge as follows,

$$\begin{aligned} \left(G^{(2)}\right)_{\mu\nu}^{ab}(p^2, \Lambda) &= \frac{G(p^2, \Lambda)}{p^2} \delta_{ab} \left(\delta_{\mu\nu} - \frac{p_\mu p_\nu}{p^2} \right), \\ \left(F^{(2)}\right)^{a,b}(p^2, \Lambda) &= -\delta_{ab} \frac{F(p^2, \Lambda)}{p^2}; \end{aligned} \quad (2.1)$$

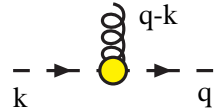
Λ being some regularisation parameter ($a^{-1}(\beta)$ if, for instance, we specialise to lattice regularisation). The renormalized dressing functions, G_R and F_R are defined through :

$$\begin{aligned} G_R(p^2, \mu^2) &= \lim_{\Lambda \rightarrow \infty} Z_3^{-1}(\mu^2, \Lambda) G(p^2, \Lambda) \\ F_R(p^2, \mu^2) &= \lim_{\Lambda \rightarrow \infty} \tilde{Z}_3^{-1}(\mu^2, \Lambda) F(p^2, \Lambda), \end{aligned} \quad (2.2)$$

with renormalization condition

$$G_R(\mu^2, \mu^2) = F_R(\mu^2, \mu^2) = 1. \quad (2.3)$$

Now, we will consider the ghost-gluon vertex which could be non-perturbatively obtained through a three-point Green function, defined by two ghost and one gluon fields, with amputated legs after dividing by two ghost and one gluon propagators. This vertex can be written quite generally as:

$$\tilde{\Gamma}_v^{abc}(-q, k; q-k) = \frac{-}{k} \rightarrow \text{diagram} \rightarrow \frac{-}{q} = ig_0 f^{abc} (q_\nu H_1(q, k) + (q-k)_\nu H_2(q, k)), \quad (2.4)$$


where q is the outgoing ghost momentum and k the incoming one, and renormalized according to:

$$\tilde{\Gamma}_R = \tilde{Z}_1 \Gamma. \quad (2.5)$$

The vertex Γ_v involves two independent scalar functions. In the *MOM* renormalization procedure \tilde{Z}_1 is fully determined by demanding that one specific combination of those two form factors (chosen at one's will) be equal to its tree-level value for a specific kinematical configuration. We choose to apply *MOM* prescription for the scalar function $H_1 + H_2$ that multiplies q_ν in eq. (2.4) and the renormalization condition reads¹

$$(H_1^R(q, k) + H_2^R(q, k))|_{q^2=\mu^2} = \lim_{\Lambda \rightarrow \infty} \tilde{Z}_1(\mu^2, \Lambda) (H_1(q, k; \Lambda) + H_2(q, k; \Lambda))|_{q^2=\mu^2} = 1, \quad (2.6)$$

where we prescribe a kinematics for the subtraction point such that the outgoing ghost momentum is evaluated at the renormalization scale, while the incoming one, k , depends on the choice of several possible configurations; for instance: $k^2 = (q-k)^2 = \mu^2$ (symmetric configuration) or $k = 0$, $(q-k)^2 = \mu^2$ (asymmetric-ghost configuration).

¹In the case of zero-momentum gluon, an appropriate choice would be $\tilde{Z}_1(\mu^2) H_1(q, q)|_{q^2=\mu^2} = 1$. This would make the renormalized vertex equal to its tree-level value at the renormalization scale.

On the other hand, the fields involved in the non-perturbative definition of the vertex Γ_v in eq. (2.4) can be directly renormalized by their renormalization constants, Z_3 and \tilde{Z}_3 , and the same MOM prescription applied to the scalar combination $H_1 + H_2$ also implies:

$$\begin{aligned} g_R(\mu^2) &= \lim_{\Lambda \rightarrow \infty} \tilde{Z}_3(\mu^2, \Lambda) Z_3^{1/2}(\mu^2, \Lambda) g_0(\Lambda^2) \left(H_1(q, k; \Lambda) + H_2(q, k; \Lambda) \right) \Big|_{q^2 \equiv \mu^2} \\ &= \lim_{\Lambda \rightarrow \infty} g_0(\Lambda^2) \frac{Z_3^{1/2}(\mu^2, \Lambda^2) \tilde{Z}_3(\mu^2, \Lambda^2)}{\tilde{Z}_1(\mu^2, \Lambda^2)}. \end{aligned} \quad (2.7)$$

We combine both eq. (2.6) and the first-line equation of (2.7) to replace $H_1 + H_2$ and obtain the second line that shows the well-known relationship $Z_g = (Z_3^{1/2} \tilde{Z}_3)^{-1} \tilde{Z}_1$, where $g_R = Z_g^{-1} g_0$.

We turn now to the specific *MOM*-type renormalization scheme defined by a **zero incoming ghost momentum**. Since those kinematics are the ones (and the only ones) in which Taylor's well known non-renormalization theorem (cf. ref [13]) is valid we shall refer to this scheme as to the *T*-scheme and the corresponding quantities will bear a *T* subscript. Then, in eq (2.4), we set k to 0 and get

$$\tilde{\Gamma}_v^{abc}(-q, 0; q) = i g_0 f^{abc} (H_1(q, 0) + H_2(q, 0)) q_v. \quad (2.8)$$

Now, Taylor's theorem states that $H_1(q, 0; \Lambda) + H_2(q, 0; \Lambda)$ is equal to 1 in full QCD for any value of q . Therefore, the renormalization condition eq. (2.6) implies $\tilde{Z}_1(\mu^2) = 1$ and then

$$\alpha_T(\mu^2) \equiv \frac{g_T^2(\mu^2)}{4\pi} = \lim_{\Lambda \rightarrow \infty} \frac{g_0^2(\Lambda^2)}{4\pi} G(\mu^2, \Lambda^2) F^2(\mu^2, \Lambda^2); \quad (2.9)$$

where we also apply the renormalization condition for the propagators, eqs. (2.2,2.3), to replace the renormalization constants, Z_3 and \tilde{Z}_3 , by the bare dressing functions. The remarkable feature of eq. (2.9) is that it involves only F and G so that no measure of the ghost-gluon vertex is needed for the determination of the coupling constant.

Equation (2.9) has extensively been advocated and studied on the lattice (see for instance reference [14]). However it must be stressed that the *T*-scheme is the **only** one in which $\tilde{Z}_1 = 1$. Nevertheless the form (2.9) is used quite often in this case (for a kinematical configuration other than *T*-scheme's) also as an approximation, specially in relation with the study of Dyson-Schwinger equations. An important remark is also in order here: in the very infrared domain, for phenomenological purposes (see for instance [15]), the coupling can be more properly defined by pulling a massive gluon propagator out from the ghost-gluon Green function used to build it [16].

2.1 Pure perturbation theory

A standard four-loop formula describing the running for the *T*-scheme coupling,

$$\begin{aligned} \alpha_T(\mu^2) &= \frac{4\pi}{\beta_0 t} \left(1 - \frac{\beta_1 \log(t)}{\beta_0^2 t} + \frac{\beta_1^2}{\beta_0^4 t^2} \left(\left(\log(t) - \frac{1}{2} \right)^2 + \frac{\tilde{\beta}_2 \beta_0}{\beta_1^2} - \frac{5}{4} \right) \right) \\ &+ \frac{1}{(\beta_0 t)^4} \left(\frac{\tilde{\beta}_3}{2\beta_0} + \frac{1}{2} \left(\frac{\beta_1}{\beta_0} \right)^3 \left(-2 \log^3(t) + 5 \log^2(t) + \left(4 - 6 \frac{\tilde{\beta}_2 \beta_0}{\beta_1^2} \right) \log(t) - 1 \right) \right) \\ &\text{with } t = \ln \frac{\mu^2}{\Lambda_T^2}. \end{aligned} \quad (2.10)$$

is obtained by inverting the β -function of α_T ,

$$\beta_T(\alpha_T) = \frac{d\alpha_T}{d\ln\mu^2} = -4\pi \sum_{i=0} \tilde{\beta}_i \left(\frac{\alpha_T}{4\pi}\right)^{i+2}; \quad (2.11)$$

where, as explained in [11], the coefficients $\tilde{\beta}_i$ can be computed in terms of $\bar{\beta}_i$, those for the β -function of the coupling renormalized according $\overline{\text{MS}}$ -scheme, $\bar{\alpha}$, and of the anomalous dimensions for gluon and ghost propagators,

$$\begin{aligned} \frac{1}{\alpha_T(\mu^2)} \frac{d\alpha_T(\mu^2)}{d\bar{\alpha}} &= \frac{1}{\beta_{\overline{\text{MS}}}(\bar{\alpha})} \left(2 \lim_{\Lambda \rightarrow \infty} \frac{d}{d\ln\mu^2} \ln F(\mu^2, \Lambda) + \lim_{\Lambda \rightarrow \infty} \frac{d}{d\ln\mu^2} \ln G(\mu^2, \Lambda) \right) \\ &= \frac{2\tilde{\gamma}(\bar{\alpha}) + \gamma(\bar{\alpha})}{\beta_{\overline{\text{MS}}}(\bar{\alpha})}. \end{aligned} \quad (2.12)$$

Both anomalous dimensions need to be renormalized along MOM prescriptions (*i.e.*, $G_R(\mu^2, \mu^2) = F_R(\mu^2, \mu^2) = 1$) but expanded in terms of $\bar{\alpha}$. The coefficients so obtained (the details and results of the computation can be found in [11]) appear to agree with those directly obtained in ref. [17] by the three-loop perturbative subtraction of the ghost-gluon-gluon vertex in the QCD Lagrangian with the appropriate kinematical configuration (T -scheme).

2.2 OPE power corrections

In order to extend the description of the running coupling down to energies as low as possible (of the order of 3 GeV) and to take full advantage of the lattice data we want to compare with, in order to reduce the systematic uncertainties, it is mandatory to take into account the gauge-dependent dimension-two OPE power corrections (*cf.* [7, 8, 10, 18]) to α_T .

The leading power contribution to the ghost propagator,

$$(F^{(2)})^{ab}(q^2) = \int d^4x e^{iq \cdot x} \langle T(c^a(x) \bar{c}^b(0)) \rangle \quad (2.13)$$

can be computed using the operator product expansion [19] (OPE), as is done in ref. [20],

$$T(c^a(x) \bar{c}^b(0)) = \sum_t (c_t)^{ab}(x) O_t(0); \quad (2.14)$$

here O_t is a local operator, regular when $x \rightarrow 0$, and the Wilson coefficient c_t contains the short-distance singularity. Eq. (2.14) involves a full hierarchy of terms, ordered according to their mass-dimension, among which only $\mathbf{1}$ and $:A_\mu^a A_\nu^b:$ contribute to eq. (2.13) in Landau gauge² up to the order $1/q^4$. Then, using eq. (2.14) into eq. (2.13), we obtain:

$$\begin{aligned} (F^{(2)})^{ab}(q^2) &= (c_0)^{ab}(q^2) + (c_2)_{st}^{ab\sigma\tau}(q^2) \langle :A_\sigma^s(0) A_\tau^t(0): \rangle + \dots \\ &= (F_{\text{pert}}^{(2)})^{ab}(q^2) + w^{ab} \frac{\langle A^2 \rangle}{4(N_C^2 - 1)} + \dots \end{aligned} \quad (2.15)$$

²The operators with an odd number of fields ($d = 1, 3/2$; $\partial_\mu A$ and $\partial_\mu \bar{c}$) cannot satisfy colour and Lorentz invariance and do not contribute a non-zero non-perturbative expectation value, and $\bar{c}c$ does not contribute either because of the particular tensorial structure of the ghost-gluon vertex.

Finally, putting together the defining relation eq. (2.9) and the results eqs. (2.17,2.20) we get

$$\begin{aligned}
\alpha_T(\mu^2) &= \lim_{\Lambda \rightarrow \infty} \frac{g_0^2}{4\pi} F^2(\mu^2, \Lambda) G(\mu^2, \Lambda) \\
&= \underbrace{\lim_{\Lambda \rightarrow \infty} \frac{g_0^2}{4\pi} F^2(q_0^2, \Lambda) G(q_0^2, \Lambda)}_{\alpha_T^{\text{pert}}(q_0^2)} F_R^2(\mu^2, q_0^2) G_R(\mu^2, q_0^2) \\
&= \underbrace{\alpha_T^{\text{pert}}(q_0^2) F_{R,\text{pert}}^2(\mu^2, q_0^2) G_{R,\text{pert}}(\mu^2, q_0^2)}_{\alpha_T^{\text{pert}}(\mu^2)} \left(1 + \frac{9}{\mu^2} \frac{g_T^2(q_0^2) \langle A^2 \rangle_{R,q_0^2}}{4(N_C^2 - 1)} \right), \quad (2.21)
\end{aligned}$$

where $q_0^2 \gg \Lambda_{\text{QCD}}$ is some perturbative scale and the running of the perturbative part of the evolution, α_T^{pert} , is of course described by the eq. (2.10) in the previous section. Again, the Wilson coefficient at leading logarithm for the T-scheme MOM running coupling is obtained in [11] and found not to induce a significant effect, provided that the coupling multiplying A^2 inside the bracket is taken to be renormalized also in T-scheme. Thus, eq. (2.21) describes pretty well the running of α_T roughly above 3 Gev.

3. Data Analysis by the “plateau” method

In the following, as done in [11], we will apply a “plateau”-procedure exploiting eq. (2.21) to get a reliable estimate of the Λ_{QCD} -parameter from lattice data. The goal being to get a trustworthy estimate of the $\Lambda_{\overline{\text{MS}}}$ -parameter, one could attempt to do it by inverting the perturbative formula eq. (2.10) and using in the *inverted* formula the lattice estimates of the running coupling obtained by means of eq. (2.9) for as many lattice momenta as possible. Then, one should look for a “plateau” of $\Lambda_{\overline{\text{MS}}}$ in terms of momenta in the high-energy perturbative regime (this was done with the coupling defined by the three-gluon vertex in [4, 5]). In the next subsection, fig. 1.(a) shows the estimates of $\Lambda_{\overline{\text{MS}}}$ so calculated for the lattice data presented in ref. [20, 22] over $9 \lesssim p^2 \lesssim 33 \text{ GeV}^2$.

However, in order to take advantage of the largest possible momenta window one can use instead eq. (2.21). In this way we shall hopefully be able to extend towards *low* momenta the region over which to look for the best possible values of the gluon condensate and of $\Lambda_{\overline{\text{MS}}}^3$. In other words, one requires the best-fit to a constant of

$$(x_i, y_i) \equiv (p_i^2, \Lambda(\alpha_i)) \quad , \quad \text{with :} \quad \alpha_i = \frac{\alpha_{\text{Latt}}(p_i^2)}{1 + \frac{c}{p_i^2}}; \quad (3.1)$$

where $\Lambda(\alpha)$ is obtained by inverting the perturbative four-loop formula, eq. (2.10), and c results from the best-fit (it appeared written in terms of the gluon condensate in eq. (2.21)). Thus, $\Lambda(\alpha)$ reaches a “plateau” (if it does) behaving in terms of the momentum as a constant that we will take as our estimate of $\Lambda_{\overline{\text{MS}}}$. Of course, this is nothing but a fitting strategy for a 2-parameters ($\Lambda_{\overline{\text{MS}}}$ and $\langle A^2 \rangle$) fit of the estimates of eq. (2.9) from lattice data.

³This increases the statistics and reduces errors. It also avoids some possible systematic deviation appearing when lattice momentum components, in lattice units, approach $\pi/2$ (Brillouin’s region border).

3.1 Results for pure Yang-Mills ($N_f = 0$)

The quenched lattice data that we will exploit now were presented for the first time in ref. [22]. We refer to this work for all the details concerning the lattice implementation: algorithms, action, Faddeev-Popov operator inversion, etc. The parameters of the whole set of simulations are described in table 1

β	Volume	a^{-1} (GeV)	Number of confs.
6.0	16^4	1.96	1000
6.0	24^4	1.96	500
6.2	24^4	2.75	500
6.4	32^4	3.66	250

Table 1: Run parameters of the exploited data.

In fig. 1.(a), we show the estimates of $\Lambda_{\overline{\text{MS}}}$ obtained when interpreting the lattice coupling computed by eq. (2.9) for any momentum $9 \lesssim p^2 \lesssim 33 \text{ GeV}^2$ in terms of the *inverted* four-loop perturbative formula for the coupling, eq. (2.10). The estimates systematically decrease as the squared momentum increases until around 22 GeV^2 ; above this value, only a noisy pattern results. In fig. 1.(b), the same is plotted but inverting instead the non-perturbative formula including power corrections, eq. (2.21). The value of the gluon condensate has been determined by requiring a “plateau” to exist (as explained in the previous section) over the total momenta window.

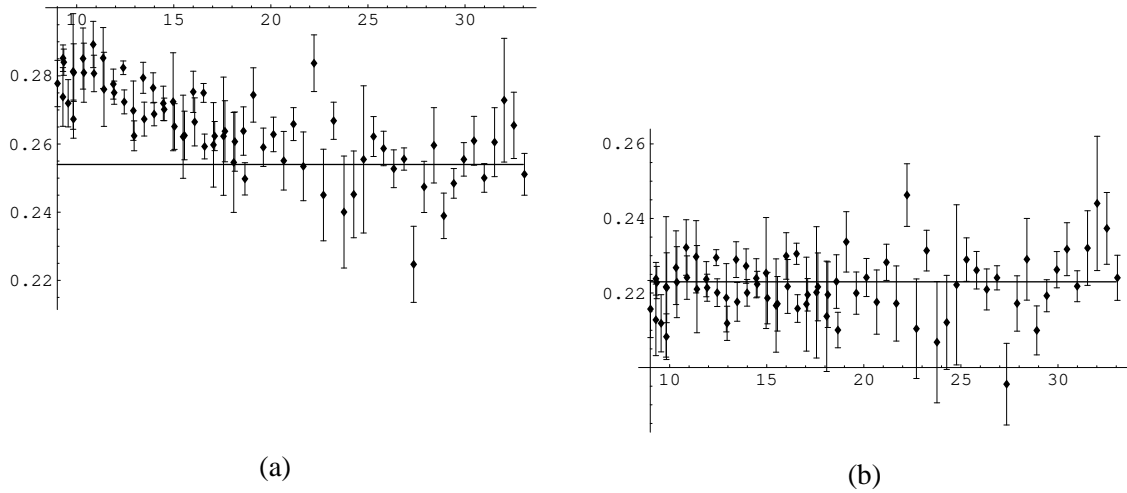


Figure 1: (a) Plot of $\Lambda_{\overline{\text{MS}}}$ (in GeV) computed by the inversion of the four-loop perturbative formula as a function of the square of the momentum (in GeV^2); the coupling is estimated from the lattice data through the perturbative formula obtained in the text. (b) Same as plot (a) except for applying the non-perturbative formula obtained in the text for the coupling and looking for the gluon condensate generating the best plateau over $9 \lesssim p^2 \lesssim 33 \text{ GeV}^2$.

One should realize that the non-perturbative analysis seems to indicate that the perturbative regime is far from being achieved at $p = 5 \text{ GeV}$. This is also illustrated by figure 2.a in which, adopting for $\Lambda_{\overline{\text{MS}}}$ the value 224 MeV which results from the non-perturbative analysis, we plot

	F^2G [11]	Asym. 3-g [8]	Sym. 3-g [8]	F/G [20]	[2]
$\Lambda_{\overline{\text{MS}}} \text{ (MeV)}$	224_{-5}^{+8}	260(18)	233(28)	270(30)	238(19)
$\sqrt{\langle A^2 \rangle}_{R,\mu} \text{ (GeV)}$	1.64(17)	2.3(6)	1.9(3)	1.3(4)	–

Table 2: Comparison of the estimate of $\Lambda_{\overline{\text{MS}}}$ obtained from the analysis of the ghost-gluon vertex (first column) and others from literature. The renormalization point is $\mu = 10 \text{ GeV}$.

against the square of the renormalization momentum the coupling constant as computed by means of the non-perturbative formula (2.21) (red curve) and of the perturbative one (2.10) (blue curve). Displayed are also the lattice data, *i.e.* the values of α_T obtained from eq. (2.9).

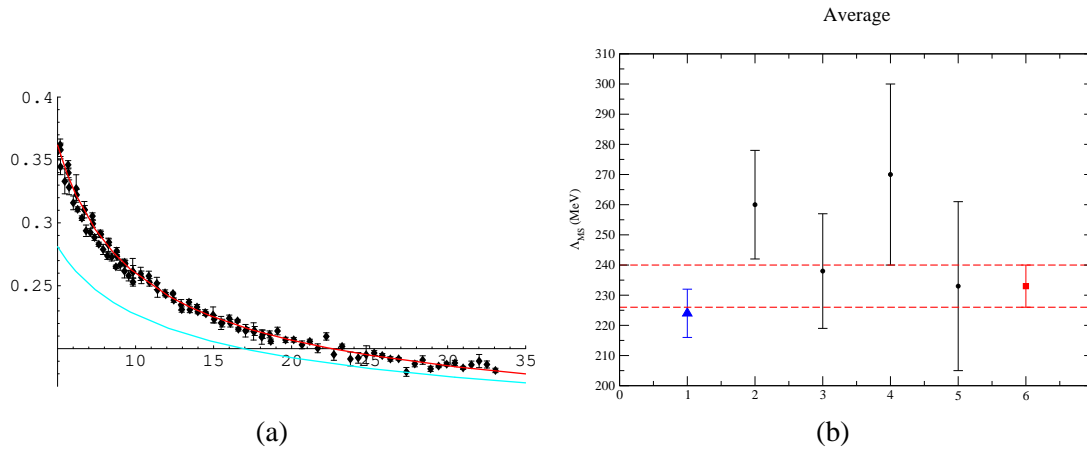


Figure 2: (a) Plot of α_T in terms of the square of the renormalization momentum: the red solid line is computed with the non-perturbative formula with $\Lambda_{\overline{\text{MS}}} = 224 \text{ MeV}$, the blue one with the perturbative one for the same $\Lambda_{\overline{\text{MS}}}$ and the data are obtained from the lattice data set-up described in the text. (b) Comparison with previous published estimates of $\Lambda_{\overline{\text{MS}}}$ in pure Yang-Mills; the blue triangle stands for the estimate in this work and the red square for the *average* of the five estimates presented in the plot.

Thus, one can conclude that our best-fit parameters incorporating only ⁴ statistical errors are:

$$\begin{aligned} \Lambda_{\overline{\text{MS}}}^{N_f=0} &= 224_{-5}^{+8} \text{ MeV} \\ g_T^2 \langle A^2 \rangle_R &= 5.1_{-1.1}^{+0.7} \text{ GeV}^2 . \end{aligned} \quad (3.2)$$

These values are in very good agreement with the previous estimates from quenched lattice simulations of the three-gluon Green function [7, 8] or, in the case of $\Lambda_{\overline{\text{MS}}}$, from the implementation of the Schrödinger functional method [2], although slightly larger than the one obtained by the ratio of ghost and gluon dressing functions [20] (see fig. 2.(b) and tab. 2).

4. About the nature and the size of the gluon condensate

The nature of the dimension-two gluon condensate, as well as its possible phenomenological implications, have been discussed in many works in the last few years (see for instance [12, 18]).

⁴The error analysis is deeply discussed in [11].

In particular, we presented some indications supporting the idea that the low-momentum gluon correlation functions could be nicely described in terms of the semiclassical instanton background for the gauge field [23], and used an instanton liquid picture to estimate the size for this gluon condensate in Yang-Mills [10]. Indeed, the gauge field in the instanton picture and within the sum-ansatz approach, can be written in the singular Landau gauge as

$$gA_\mu^a = 2 \sum_i R^{a\alpha} \bar{\eta}_{\mu\nu}^\alpha \frac{(x^\nu - z_\nu^i)}{|x - z^i|^2} \phi \left(\frac{|x - z^i|}{\rho_i} \right), \quad (4.1)$$

where $g = (6/\beta)^{1/2}$ is the bare gauge coupling in terms of the lattice parameter β , $\bar{\eta}$ is known as 't Hooft symbol and $R^{a\alpha}$ represents the color rotations embedding the canonical SU(2) instanton solution in the SU(3) gauge group, $\alpha = 1, \dots, 3$ ($a = 1, \dots, 8$) being an SU(2) (SU(3)) color index. The sum is extended over all the instantons and anti-instantons (we should then replace the 't Hooft symbol $\bar{\eta}$ by η) in the classical background of the gauge configuration. $\phi(x)$ is the instanton profile function. If we consider the profile of the BPST solution for an isolated instanton, we get

$$g^2 \langle A^2 \rangle \equiv \frac{N_I + N_A}{V} \int d^4x \sum_{\mu,a} gA_\mu^a gA_\mu^a = 12\pi^2 \rho^2 \frac{N_I + N_A}{V} = 12\pi^2 \rho^2 n; \quad (4.2)$$

where N_I (N_A) stands for the total number of instantons (anti-instantons). On the other hand, if we neglect instanton position and color correlations, eq. (4.1) leads for the m -gluon Green function to

$$G^{(m)}(k^2) = n \frac{4k^2}{m} \left(\frac{\beta}{96k^2} \right)^{m/2} \langle \rho^{3m} I(k\rho)^m \rangle, \\ \text{where } I(s) = \frac{8\pi^2}{s} \int_0^\infty dz z J_2(sz) \phi(z), \quad (4.3)$$

for $m = 2, 3$; n being the instanton density. It depends on the functional $I(k\rho)$ of the general instanton profile, $\phi(x)$, and $\langle \dots \rangle$ means the average over instanton sizes with a given normalised instanton radius distribution, $\mu(\rho)$. Then, two interesting limits appear where some results not depending on the instanton profile can be obtained:

- For a sharp radius distribution, the particular combination of two and three-gluon Green functions defining the three-gluon running coupling in ref. [5] gives [24]

$$\alpha_{3g}(k^2) = \frac{k^6}{4\pi} \frac{(G^{(3)})^2}{(G^{(2)})^3} = \frac{k^4}{18\pi n}; \quad (4.4)$$

- For $k\rho \gg 1$, as $I(s)$ asymptotically behaves as $16\pi^2/s^3$ in the large s limit, one obtains

$$G^{(m)}(k^2) \simeq n \frac{4}{m} \left(\frac{8\beta}{3} \right)^{m/2} k^{2-4m}. \quad (4.5)$$

Thus, eq. (4.5) provides us with large-momentum limits for the two and three-gluon Green functions behaviour which do not depend on the radius distribution nor on the instanton profile. However, the large-momentum lattice correlation function being dominated by the short-distance quantum fluctuations, whether such a behaviour occurs can be only detected after performing some

“cooling” procedure [25] to kill the higher energy modes. This is done in [23] and, as can be seen in fig. 3.a, the expected k^{-6} (k^{-10}) power behaviour clearly emerges for the two-gluon (three-gluon) Green function after “cooling”. This is a good indication for the success of the instanton picture in describing the gluon correlation functions. However, as the “cooling” has been proved to alter the configuration (instanton sizes become distorted, instanton and anti-instanton annihilate to each other...), the power-law given by eq. (4.4), which is thought to be followed by the “uncooled” gluon correlators in the low-momentum regime, offers a more reliable “instanton detector”. In ref. [24], eq. (4.4) is shown to work for a three-gluon coupling computed from several lattice simulations (see fig. 3.b taken from [24]) and the instanton density is estimated to be $n \simeq 5 \text{ fm}^{-4}$.

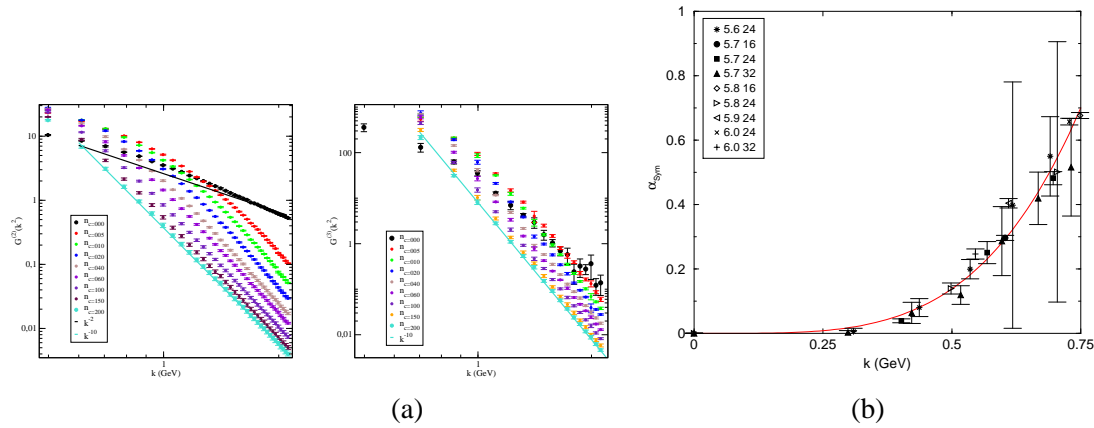


Figure 3: (a) two and three-gluon Green functions after cooling: they reach their expected power-law when the number of cooling sweeps increases. (b) The three-gluon coupling defined in the text: it follows the expected low-momentum k^4 power-law with $n = 5.27(4) \text{ fm}^{-4}$.

Then, this estimate of the instanton density and the average instanton radius, $\bar{\rho} \simeq 0.4 \text{ fm}$ (measured, for instance, in [23] and being close to the phenomenological prediction, $\simeq 1/3 \text{ fm}$), can be applied to eq. (4.2) to give: $g^2 \langle A^2 \rangle \simeq 4 \text{ GeV}^2$. There is of course no exact recipe to compare this estimate with the OPE one, since the separation between the semiclassical non perturbative domain and the perturbative one cannot be exact⁵. However, both lie prettily on the same ballpark.

5. Conclusion

We have demonstrated that, in the particular T -scheme, the coupling defined from the ghost-gluon vertex is obtained by only dealing with two-point Green functions. Some interesting non-perturbative information can be furthermore distilled from the running analysis of this coupling beyond the deep IR: the Λ_{QCD} parameter (usually expressed in the $\overline{\text{MS}}$ -scheme), computed here for pure Yang-Mills from Landau gauge lattice simulations, and a gauge-dependent dimension-two gluon condensate. The latter is interpreted and sized by invoking an instanton liquid picture, which successfully describes the low-momentum gluon correlations.

⁵One may appeal to the fact that at the renormalisation point μ , the radiative corrections are minimised; therefore a semiclassical estimate must best correspond to $\langle A^2 \rangle_{\text{R},\mu}$ at some reasonable μ , which one could guess to be a typical scale of the problem as $1/\rho$ or some gluon mass.

References

- [1] G. S. Bali and K. Schilling, Phys. Rev. D **47** (1993) 661 [arXiv:hep-lat/9208028].
- [2] M. Luscher, R. Sommer, P. Weisz and U. Wolff, Nucl. Phys. B **413** (1994) 481; S. Capitani, M. Luscher, R. Sommer and H. Wittig [ALPHA Collaboration], Nucl. Phys. B **544** (1999) 669
- [3] G. M. de Divitiis, R. Frezzotti, M. Guagnelli and R. Petronzio, Nucl. Phys. B **433** (1995) 390
- [4] B. Alles *et al.* Nucl. Phys. B **502** (1997) 325 [arXiv:hep-lat/9605033].
- [5] P. Boucaud, J. P. Leroy, J. Micheli, O. Pène and C. Roiesnel, JHEP **9810** (1998) 017
- [6] P. Boucaud *et al.*, JHEP **0004** (2000) 006 [arXiv:hep-ph/0003020].
- [7] Ph. Boucaud, A. Le Yaouanc, J.P. Leroy, J. Micheli, O. Pène, J. Rodriguez-Quintero, Phys. Lett. **B493**(2000) 315.
- [8] Ph. Boucaud, A. Le Yaouanc, J.P. Leroy, J. Micheli, O. Pène, J. Rodriguez-Quintero, Phys. Rev. D **63**(2001) 114003; F. De Soto and J. Rodriguez-Quintero, Phys. Rev. D **64** (2001) 114003 .
- [9] A. Sternbeck, K. Maltman, L. von Smekal, A. G. Williams, E. M. Ilgenfritz and M. Muller-Preussker, PoS **LAT2007** (2007) 256 [arXiv:0710.2965 [hep-lat]].
- [10] P. Boucaud *et al.*, Phys. Rev. D **66** (2002) 034504; JHEP **0304** (2003) 005; Phys. Rev. D **70** (2004) 114503.
- [11] Ph. Boucaud *et al.*, Phys. Rev. D **79** (2009) 014508 [arXiv:0811.2059 [hep-ph]].
- [12] F. V. Gubarev and V. I. Zakharov, Phys. Lett. B **501** (2001) 28 [arXiv:hep-ph/0010096].
- [13] J. C. Taylor, Nuclear Physics B33 (1971) 436
- [14] L. von Smekal, R. Alkofer and A. Hauck, Phys. Rev. Lett. **79** (1997) 3591 [arXiv:hep-ph/9705242].
- [15] D. Binosi and J. Papavassiliou, Phys. Rept. **479** (2009) 1 [arXiv:0909.2536 [hep-ph]].
- [16] A. C. Aguilar, D. Binosi, J. Papavassiliou and J. Rodriguez-Quintero, Phys. Rev. D **80** (2009) 085018
- [17] K. G. Chetyrkin and A. Retey, [arXiv:hep-ph/0007088]; T. van Ritbergen, J. A. M. Vermaseren and S. A. Larin, Phys. Lett. B **400** (1997) 379.
- [18] D. Dudal, H. Verschelde and S. P. Sorella, Phys. Lett. B **555** (2003) 126 ; K. I. Kondo, Phys. Lett. B **572** (2003) 210 ; [arXiv:hep-th/0306195].
- [19] R. Wilson, Phys. Rev. **179** (1969) 1499.
- [20] Ph. Boucaud *et al.*, JHEP **0601** (2006) 037 [arXiv:hep-lat/0507005]; Phys. Rev. D **63**(2001) 114003.
- [21] M.A. Shifman, A.I. Vainshtein, V.I. Zakharov, Nucl. Phys. B **147**(1979) 385; M.A. Shifman, A.I. Vainshtein, M.B. Voloshin, V.I. Zakharov, Phys. Lett. B **77**(1978) 80.
- [22] Ph. Boucaud *et al.*, Phys. Rev. D **72** (2005) 114503 [arXiv:hep-lat/0506031].
- [23] Ph. Boucaud *et al.* JHEP **0503** (2005) 046 ; Phys. Rev. D **70** (2004) 114503.
- [24] P. Boucaud *et al.*, JHEP **0304** (2003) 005 [arXiv:hep-ph/0212192].
- [25] M. Teper, Phys. Lett. B **162** (1985) 357.